doi 10.4436/jass.94019

JASs *Proceeding Paper*

Journal of Anthropological Sciences
Vol. 94 (2016), pp. 41-63

Filling the gap. Human cranial remains from Gombore II (Melka Kunture, Ethiopia; ca. 850 ka) and the origin of *Homo heidelbergensis*

Antonio Profico[1], Fabio Di Vincenzo[1], Lorenza Gagliardi[1], Marcello Piperno[2] & Giorgio Manzi[1]

1) Sapienza Università di Roma, Dipartimento di Biologia Ambientale, P.le Aldo Moro 5, 00185 Roma, Italy
e-mail: giorgio.manzi@uniroma1.it

2) Sapienza Università di Roma, Dipartimento di Scienze dell'Antichità, P.le Aldo Moro 5, 00185 Roma, Italy

Summary - *African archaic humans dated to around 1,0 Ma share morphological affinities with* Homo ergaster *and appear distinct in cranio-dental morphology from those of the Middle Pleistocene that are referred to* Homo heidelbergensis. *This observation suggests a taxonomic and phylogenetic discontinuity in Africa that ranges across the Matuyama/Brunhes reversal (780 ka). Yet, the fossil record between roughly 900 and 600 ka is notoriously poor. In this context, the Early Stone Age site of Gombore II, in the Melka Kunture formation (Upper Awash, Ethiopia), provides a privileged case-study. In the Acheulean layer of Gombore II, somewhat more recent than 875±10 ka, two large cranial fragments were discovered in 1973 and 1975 respectively: a partial left parietal (Melka Kunture 1) and a right portion of the frontal bone (Melka Kunture 2), which probably belonged to the same cranium. We present here the first detailed description and computer-assisted reconstruction of the morphology of the cranial vault pertaining to these fossil fragments. Our analysis suggest that the human fossil specimen from Gombore II fills a phenetic gap between* Homo ergaster *and* Homo heidelbergensis. *This appears in agreement with the chronology of such a partial cranial vault, which therefore represents at present one of the best available candidates (if any) for the origin of* Homo heidelbergensis *in Africa.*

Keywords - *Paleoanthropology, Human evolution, Geometric Morphometrics, Bézier curve, Matuyama/Brunhes boundary, Africa.*

Introduction

The human fossil record bracketed between roughly 900 and 600 ka in sub-Saharan Africa is notoriously poor. Earlier cranial specimens such as the calvaria known as Daka in the Ethiopian region of the Middle Awash (Asfaw *et al.*, 2002, 2008), the cranium from Buia in the Eritrean Danakil depression (Abbate *et al.*, 1998; Macchiarelli *et al.*, 2004) and the cranial bone fragments from Olorgesailie in Kenya (Potts *et al.*, 2004), all dated around 1,0 Ma, share morphological affinities with *Homo ergaster*, despite signs of an advanced degree of encephalisation, with enlarged braincase and more vertical parietal walls.

At the same time, these African specimens of the late Early Pleistocene are different from those of the Middle Pleistocene that exhibit, in Africa as elsewhere, a variable combination of archaic and derived morphologies, including further broadening of the cranial vault, less flattened midsagittal profile, peculiar morphology of the supraorbital torus (e.g., Rightmire, 1998; Mounier *et al.*, 2011; Stringer, 2012). Humans of the Middle Pleistocene are therefore commonly ascribed to a different species referred to as *Homo heidelbergensis*. In a more

speciose scenario, as far as the African fossil record is concerned, the *nomen Homo rhodesiensis* applies to specimens such as Bodo, Kabwe and Saldanha (or Elandsfontein), which are followed by more derived humans that are sometimes referred to another different deme (corresponding, at least in part, to the controversial *Homo helmei*; see Rightmire, 2009), from which *Homo sapiens* probably emerged.

The taxonomic discontinuity occurring in Africa at the boundary between Early and Middle Pleistocene has a counterpart in Europe with the disappearance of *Homo antecessor*, as it has been described on the sample from Gran Dolina of Atapuerca in Spain (Bermudez de Castro *et al.*, 1997), followed by the diffusion of a new kind of humans bearing the Acheulean and commonly referred to (not without controversies; e.g., Balter, 2014) *Homo heidelbergensis*. Therefore, the time span around the Matuyama/Brunhes reversal of 780 ka should be regarded as crucial for human evolution (Manzi *et al.*, 2011), as it is also suggested by inferences based on mtDNA data (e.g., Krause *et al.*, 2010; Green *et al.*, 2008).

In this context, one of the localities in the Melka Kunture area (Upper Awash, Ethiopia) provides some relevant fossil remains. This is the Acheulean site of Gombore II, dated to about 850 ka, where two large cranial fragments were found in 1973 and 1975 respectively. Since their discovery, these fossil specimens have been considered as belonging to the same cranium and provide evidence for significant components of the morphology of the parietal and frontal bones respectively. In this paper, we provide the first detailed description of the two human specimens from Gombore II, a geometric-morphometric comparative analysis of their phenetic affinities, and a computer-assisted reconstruction of the morphology of the braincase that the two cranial fragments represent.

Gombore II

The site

Gombore II is in the Melka Kunture archaeological area, which extends for about 6 km in the upper Awash Valley, at about 50 kilometres south of Addis Ababa, Ethiopia (Oromia Region, 8°41′0″N - 37°38′0″E), and at an altitude higher than 2,000 m above sea level (Fig. 1). As a result of excavations carried out between 1970 and 1985 under the direction of Jean Chavaillon (Chavaillon & Berthelet, 2004), two distinct stratigraphic horizons have been recognized, with dating bracketed between 875 ± 10 and 709±13 ka (Morgan *et al.*, 2012). The oldest date was found in localities 1, 3-5, over a volcanic layer called "Tuff B". The more recent date was found only in the locality 2, which is also known as the "butchery site".

The abundant stone tools referred to the Acheulean are mainly made of volcanic raw materials (Chavaillon & Berthelet, 2004; Gallotti et al., 2010). These include bifaces, cleavers, flakes and some choppers. Typical are the so-called "twisted handaxes" (Chavaillon & Berthelet, 2004; Gallotti et al., 2010) which are made of obsidian. These bifacial tools are of particular interest because they are almost unknown elsewhere in East Africa (Chavaillon, 1979) and show affinities with Lower Palaeolithic assemblages from England (White, 1998). Gombore II looks quite poor from a palynological perspective, but for the occurrence of Gramineae (Bonnefille, 1972). In contrast, the faunal fossil record is rich and includes: *Hippopotamus* cf. *amphibius*, *Diceros bicornis*, *Stylohipparion* sp., *Hipparion* sp., *Equus* cf. *mauritanicum*, *Pelorovis oldowayensis*, *Connochaetes* cf. *taurinus*, *Damaliscus niro*, *Kobus* cf. *kob*, *Gazella* sp., *Metridiochoerus compactus*, *Giraffa* cf. *jumae*, T*achyoryctes konjiti*, *Hyaena hyaena*, *Canis* sp. and *Tadorna* sp. (Geraads, 1979, 1985; Chavaillon & Coppens, 1986; Gallotti et al., 2010).

Dating

The current chronology of more than 70 archaeological layers identified thus far in the Melka Kunture area was based on $^{40}Ar/^{39}Ar$ dating (Morgan *et al.*, 2012). Among the layers analysed at Gombore II (Fig. 1), the unit 9959 is of particular interest because immediately below the Acheulean level (unit 9958) where the human

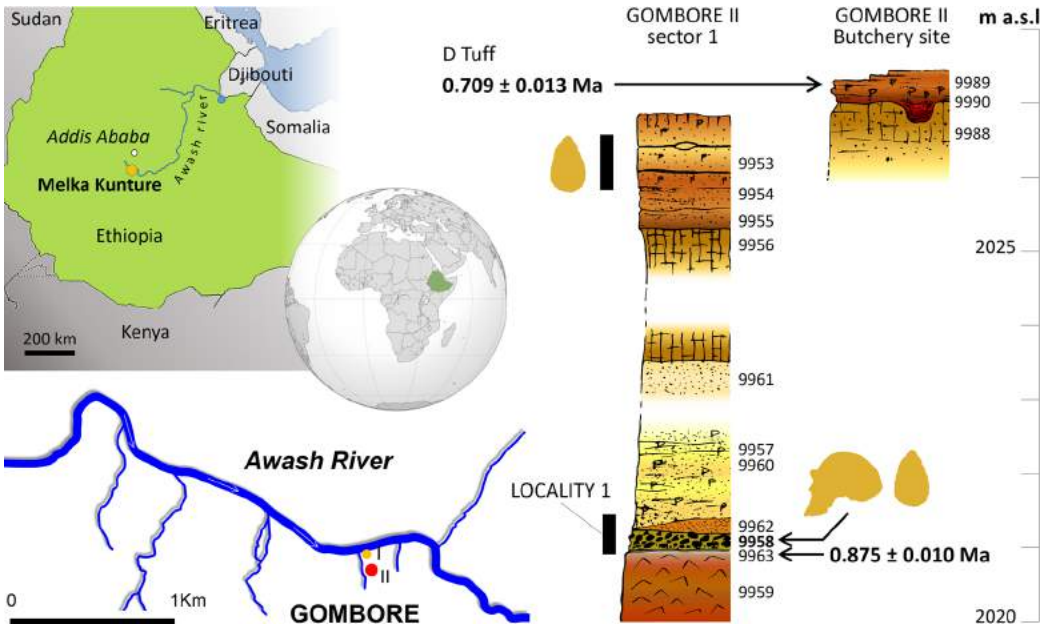

Fig. 1 - Geographical location of the Gombore sites I and II (where fossil human specimens of different chronologies were discovered; compare Di Vincenzo* et al.*, 2015) within the Melka Kunture area, south of Addis Ababa, Ethiopia. On the right, the stratigraphic section of Gombore II (modified from Raynal* et al.*, 2004), with 40Ar/39Ar ages from Morgan and colleagues (2012). The archaeological levels (Acheulean) and the position of the human fossil specimens (cranial pieces) are indicated. Numbers from 9953 to 9990 refer to the stratigraphic units described by Raynal and colleagues (2004). The colour version of this figure is available at the JASs website.

remains were found. It is composed of a fine-grained white volcanic ash that gave a $^{40}Ar/^{39}Ar$ date of 875 ± 10 ka, while samples taken from the top of the sequence at locality 2 have provided a date of 709 ± 13 ka. The stratigraphic position of the human remains from Gombore II fits the chronological range interposed between these two dates, but it is closer to the older one, suggesting a tentative chronology for the human fossils somewhat younger than 875 ka.

Paleomagnetic data support this interpretation (Tamrat *et al.*, 2014). The normal polarity (Brunhes) of the higher layers of Gombore II changes soon along the stratigraphic column, pointing to a time span preceding the Matuyama/Brunhes reversal, thus earlier than 780 ka, for the underlying levels including unit 9958. In conclusion, a reasonable chronology for the stratigraphic position of the human remains should be considered as bracketed between 780 and 875 ka, closer to the latter limit, thus ranging around 850 ka.

The human remains

In 1973, during excavations in the Acheulean levels of locality 1, Claude Brahimi unearthed a partial left parietal, labelled MK73/GOM II - 6769 and formally referred to as Melka Kunture 1 (Oakley *et al.*, 1977), hereafter MK1. When discovered the find appeared strongly mineralized and encrusted with sandy material. It was classified as *Homo* cf. *erectus* (Chavaillon *et al.*, 1974; Chavaillon & Coppens, 1975, 1986) as it is also reported in the subsequent literature

(e.g., Schwartz & Tattersal, 2005; Chavaillon & Berthelet, 2004; Coppens, 2004).

Two years later (1975), Rhorissa Delessa found a portion of human frontal bone just a few meters downstream of the area of excavation, in a narrow gorge that runs through the site with a seasonal stream (Chavaillon & Coppens, 1986). It was labelled MK76/GOM II - 576 (formally Melka Kunture 2, or MK2). Even according to the most recent interpretations (e.g., Chavaillon & Berthelet, 2004), it is likely that MK2 originated from the same layer where MK1 was previously found and was washed downstream by rain. The state of fossilization of the two finds, the patina and some morphological characteristics (the bone thickness in particular) provide evidence in support of this conclusion.

We directly examined the two original specimens at the National Museum of Ethiopia. These observations were integrated with the analysis of photographic documentation, high quality casts made by the Paleoanthropology Laboratory of the same museum, and CT digital data recorded in Addis Ababa.

Melka Kunture 1 (MK73 / GOM II – 6769)

MK1 is a left parietal (Fig. 2), with missing areas of bone laterally and anteriorly. It appears massive, with considerable thickness varying from a maximum of 14.23 mm to a minimum of 5.85 mm. The sub-triangular apex facing the anatomical position of the temporal squama is bounded by fractures that represent the lateral margins of the specimen. These fractures exhibit sharp edges (Fig. 2), whereas the more anterior border appears floated (Fig. 2). Even the external and the endocranial surfaces are not eroded. Posteriorly, *lambda* is preserved, together with segments of both the sagittal suture (for a length of 71.5 mm) and the lambdoid suture (35,0 mm). Both sutures retain part of their indentations, whose incompleteness is probably due to synostosis, rather than to post-depositional damage. The synostosis is most evident on the endocranial margin of the posterior tract of the sagittal suture (obelic region), suggesting an age at death of the individual about 35-40 years, if compared to *Homo sapiens* standards (Meindl & Lovejoy, 1985).

Although the parietal is incomplete anteriorly, the anterior apex of the fragment would have been close to the coronal suture, as demonstrated by the reduction in thickness of the diploe and associated blending of the external and internal layers of compact bone visible along the fracture (see Fig. 2). The length of the squama, measured parasagittally from this preserved portion close to the coronal suture to the corresponding margin along the lambdoidal suture, is 104.65 mm. In general, the diploe is strongly mineralized by infiltration, which confers a dark colour to it.

A short stretch of the temporal lines is visible on the external surface between the two major lateral fractures, in the area of greater convexity of the bone. The temporal lines run more medially than the parietal eminence (i.e. the most prominent segment of the profile in coronal section). Posteriorly, in correspondence of the preserved portion of the sagittal suture (obelic region) the bone is visibly flattened, both longitudinally and parasagittally. The parietal foramen is absent (Fig. 2).

The endocranial surface (Figs. 2, 3) includes impressions of the supero-lateral portions of the left parietal lobe, along with faint adjoining parts of the endocranial surface towards the postcentral gyrus (anteriorly) and the supramarginal gyrus (inferiorly). It is possible to recognise the posterior portion of the superior sagittal sinus as well as convolutions of both the superior and inferior parietal lobule (Fig. 3). The parietal lobe appears flat with a large depressed parasagittal area in correspondence of the superior parietal lobule. Also visible are impressions of the vascular middle meningeal system, represented by several deep branches almost reaching the sagittal edge of the bone. In particular, an anterior, rather isolated and deep groove is attributable to the bregmatic branch, while several anastomosing tracks related to the obelic branch occur more posteriorly. Only a brief impression of the lambdatic branch is visible, as the parietal angle is missing (Fig. 3). The prevalence of the obelic or middle branch has to be remarked.

Fig. 2 - Exocranial and endocranial surfaces of the left parietal bone MK 1 (MK 73/GOM II 6769). The section of the anterior-lateral fracture (a) and of the preserved portion of the sagittal suture (b) are reported below, while in the box it is shown a detail of the floated margins along the anterior fracture. The colour version of this figure is available at the JASs website.

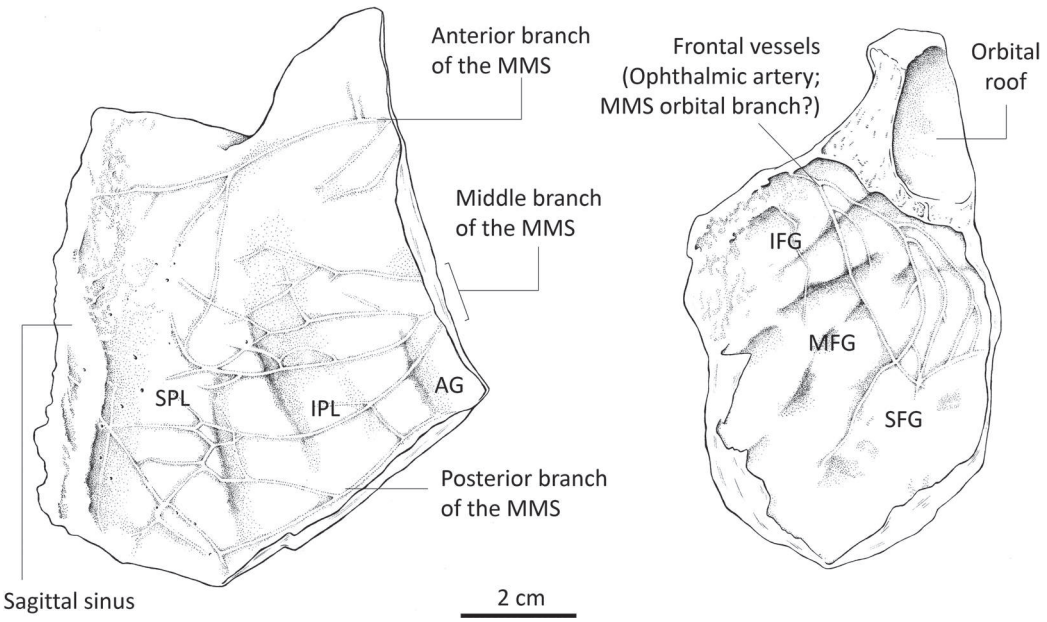

Fig. 3 - Representation of the endocranial surfaces of MK1 and MK2 showing the vascular patterns and the main cortical features. Legend: MMS = middle meningeal system; SPL = superior parietal lobule; IPL = inferior parietal lobule; AG = angular gyrus; IFG = inferior frontal gyrus; MFG = middle frontal gyrus; SFG = superior frontal gyrus.

Melka Kunture 2 (MK76 / GOM II – 576)

MK2 is a portion of the frontal bone (Fig. 4), which preserves a large part of the right side of the squama and associated components of both the orbital roof and an incomplete frontal trigone, including the lateral wing of the torus and the zygomatic process with part of the zygomaticofrontal suture.

This specimen is massive, and considerably thick. A maximum thickness of 18.12 mm and a minimum of 6.87 mm were both measured on the squama, just behind the supraorbital region excluding the preserved part of the torus. The fracture close to the mid-sagittal plane has an irregular outline but a plain section, particularly in the more anterior portion (Fig. 4), which appears rather fresh, i.e. not affected by taphonomic processes. The wide exposure of the internal structure of the bone shows that the diploe prevails over the inner and outer tables of compact bone. By contrast, the posterior fracture (toward the coronal margin of the bone) is affected by deep chipping of the outer surface, with oblique exposure of the underlying trabecular tissue. The coronal suture is not preserved, nor is most of the supraorbital torus (medial component of the trigone and the entire supraciliar arch; Cunningham, 1908) and the glabellar region. The frontal sinuses are missing.

The supraorbital torus, judging by the size of the preserved portion (with a minimum thickness of 11.22 mm, measured in correspondence of the fracture involving the roof of the orbit), appears massive and laterally expanded. The post-orbital constriction appears marked and the supratoral sulcus shallow; with respect to it, the scale rises with modest inclination, while the external profile of the bone is gently and uniformly convex. Laterally, on the external surface, the temporal lines are clearly visible and characterized by a deep sub-triangular gap (Fig. 5). The two lines, in fact, double soon in an inferior line, which originates from the posterior margin of the zygomatic process and continues nearly

Fig. 4 - The partial frontal bone MK 2 (MK 73/GOM II 6769): exocranial and endocranial surfaces. The colour version of this figure is available at the JASs website.

horizontal, and a clearly distinguished superior line, which diverges upward until a maximum separation (as far as the squama is preserved) of about 12.5 mm.

The endocranial surface (Figs. 3, 4) includes impressions of the anterior and medial portions of the right frontal lobe. It does not exhibit clear traces of the sagittal sinus and/or the frontal crest (given that the corresponding region of the bone is not preserved anteriorly), making difficult the secure identification of the sagittal plane. The superior and middle frontal gyri are well discerned, while only the more rostral portion of the inferior frontal gyrus is preserved (Figs. 3, 4); the frontal bec and the orbital portion are missing. Vascular impressions are also visible: in particular, there are five small branches transversally oriented, which we consider as vessels of the ophthalmic artery with the possible contribution of the orbital branch of the middle meningeal system (Saban, 1995). The position of the encephalic volumes appears posterior to the roof of the orbits.

Comparative samples

In the Appendix, a complete list of comparative samples used in the various analyses performed in this paper is reported. The analyses involved features of both the parietal and the frontal bone, with reference to various extinct species or operational taxonomic units (OTUs) of the genus *Homo* – *Homo ergaster* (ERG), *Homo erectus* (ERE), *Homo heidelbergensis* (see below) and *Homo neanderthalensis* (NEA) – as well as to recent samples of *Homo sapiens* (SAP). We differentiated the representatives of *Homo heidelbergensis* in macro-regional OTUs – African (HAF), Asian (HAS) and European (HEU) – and, when possible, we made also a distinction between two evolutionary "grades" among the African specimens of the Middle Pleistocene, respectively referred to as HA1 and HA2 according to their chronology and morphology.

There is one (at least) controversial issue in this respect, regarding the attribution of specimens from Atapuerca Sima de los Huesos to *Homo heidelbergensis*, given that this impressive

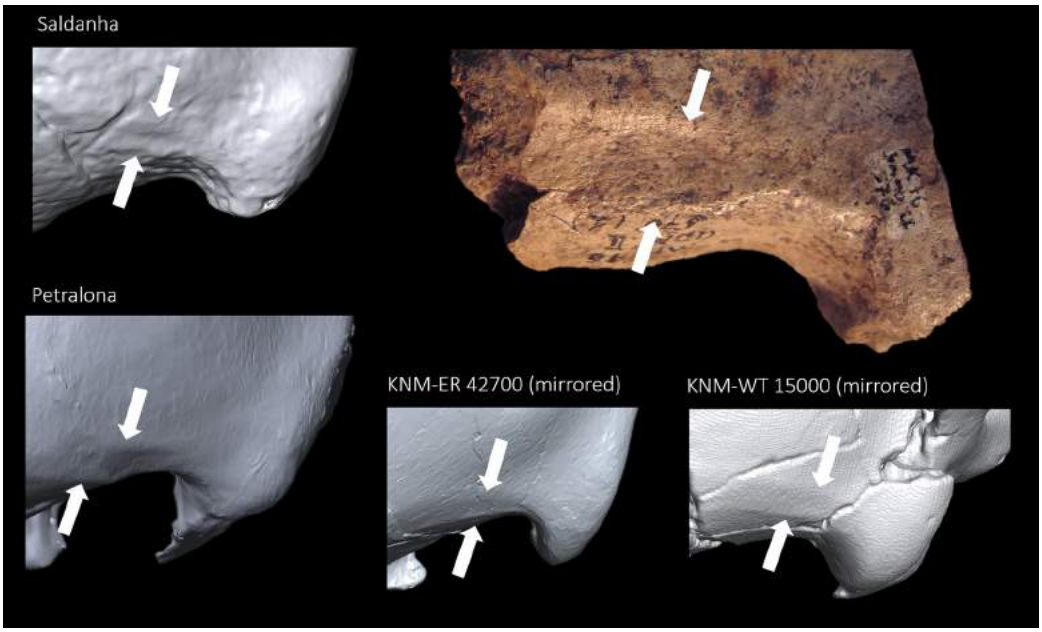

Fig. 5 - Detail of the temporal lines on MK2, diverging in the superior and inferior components since the frontal bone (arrows). This character is uncommon in both archaic and modern humans; digital comparisons (not at the same scale) are reported: Saldanha (top-left), Petralona (bottom-left), KNM-ER 42700 (bottom-centre), KNM-WT 15000 (bottom-right). The colour version of this figure is available at the JASs website.

sample (e.g., Arsuaga *et al*., 2014, 2015) shows to belong to the Neanderthal lineage more clearly than other European fossils of the same age (e.g., Hublin, 2009; Stringer 2012). Nevertheless, following previous analyses (Mounier *et al*., 2009, 2011) and reviews of the available fossil and molecular evidence (e.g., Manzi, 2004, 2012), we claim for a less speciose interpretation of the variability exhibited by African and Eurasian hominins of the Middle Pleistocene and support their common allocation within a single taxon, despite the apparent divergence in regional demes (or subspecies) that increases over time.

Methods and Results

Parietal: mid-sagittal curvature (traditional morphometrics)

Since MK1 lacks the anterior part of the sagittal suture, four values of its parietal arc and chord were estimated. For this purpose, data referring to arc and chord lengths in different samples were used to explore size and shape of the biparietal profile along the mid-sagittal plane.

As reported in Figure 6A, the arc length in MK1 was considered intermediate between the variability of *Homo ergaster* (mean = 96.29 mm; s.d. = 8.89 mm) and that of African *Homo heidelbergensis* (mean = 123.17 mm; s.d. = 7.20 mm). This suggested that the more probable estimate lies between 96 mm and 123 mm. Then, we chose four different simulations with respect to a selection of pertinent African samples, that is the following mean values: 96.0 mm (ERG; MK1a), 103.0 mm (intermediate arc length between Buia and Daka; MK1b), 121.0 mm (HA1 subsample; MK1c), and 123.0 mm (HAF; MK1d). The estimated figures of MK1 were then compared to those of 88 specimens of different species/OTUs of *Homo*. Comparative data (see Appendix) where obtained either from digital models or from

first-quality casts, integrated with data available in the literature; on digital models (both CT and laser scan), measurements were acquired through the function "SurfacePathSet" of Amira 5.4.5, using a plane-cut connector. On these bases, the chord value gave a measurement of size (Fig. 6A), while the parietal index (chord/arc length; Fig. 6B) furnished the mean curvature of the parietal bone along the midsagittal profile.

As shown in Figure 6B, *Homo neanderthalensis* and *Homo sapiens* are quite different from all the other OTUs, with the exception (at least in part) of the OTUs of *Homo heidelbergensis* (HA1 and HA2), whereas *Homo erectus* and *Homo ergaster* show lower degrees of curvature. The parietal indexes for MK1a and MK1b (estimated on *Homo ergaster*) are higher than means observed for all the other OTUs, entailing a low mean curvature value of the parietal bone along the mid-sagittal plane. In contrast, the two simulations performed on African *Homo heidelbergensis* (MK1c and MK1d) exhibit a parietal curvature intermediate between the means of ERG and HA1.

Parietal: mid-sagittal profile (geometric morphometrics)

In order to capture other components of the shape variation, as far as the mid-sagittal biparietal arc is concerned, a PCA on 49 evenly-spaced landmarks was performed (Fig. 6C) on a sample of 65 specimens belonging to *Homo ergaster*, *Homo erectus*, *Homo heidelbergensis*, *Homo neanderthalensis* and *Homo sapiens* (see Appendix). The 49 landmarks where defined as evenly-spaced points, after applying a Bézier curve (Olsen, 2014) on the original point set acquired for each specimen (Profico & Veneziano, 2015); the defined curve starts from *bregma* and ends to *lambda*. The data set was acquired either using the function "SurfacePathSet" of Amira 5.4.5 on high-resolution digital model, or a Microscribe (model G2X; time auto plot = 10 ms).

As for MK1, we calculated how many points would be missing (*mp*) in the four different simulations of the MK1 arc length described above, that is respectively close to mean values of the following African samples: ERG (MK1a: *mp* = 13), Buia and Daka (MK1b; *mp* = 15), HA1 subsample (MK1c: *mp* = 20) and HAF (MK1d; *mp* = 21). The missing points (Arbour & Brown, 2014) were estimated using a subsample belonging to HAF, HEU, and ERG, through the function "fixLMtps" of the "R" Morpho package (Schlager, 2014). The resultant 49 landmarks were used to calculate by an iterative process (i = 3) the intermediate points (N = 385), using the function "dec.curve" of the "R" Arothron package (Profico & Veneziano, 2015). The new matrix of points were used to define the final four evenly-spaced landmark sets for MK1.

The 3D landmark set of each specimen was aligned placing the origin on the *bregma* and the z axis along the mid-sagittal plane; the 3D data set was then projected in 2D, in order to remove any positional noise along the mid-sagittal plane, and a Principal Component Analysis (PCA) was finally performed on the Procrustes coordinates (69 configurations).

The first two PCs explains cumulatively more than 90% of the total variance (Fig. 6C). In this framework, as expected, the cluster of *Homo sapiens* (SAP) is clearly separated by the remaining OTUs, occupying a morpho space defined for positive values of PC1 and neutral of PC2; by contrast, other groups show negative values for PC1, in particular ERE, ERG and HAF. As for the MK1 simulations, all of them have high values for PC2, while for PC1 both MK1a and MK1b display more negative values than those of MK1c, and MK1d.

The first principal component (PC1) mainly detects parietal curvature (Fig. 6E), recording the mean curvature of the parietal arc, as highlighted by the linear regression with the parietal index (R^2=0.96, p-value=<0.001) whose values are reported in Figure 6B. PC2 deals with the flattening along the obelic trait of the biparietal profile (Fig. 6E, positive values of PC2). MK1c and MK1d are near the mean values of ERG and HAF variability along the PC1, while on PC2 they are close to African specimens of different taxonomy, being characterized by strong obelic flattening (such as Kabwe 1). We assume therefore that these

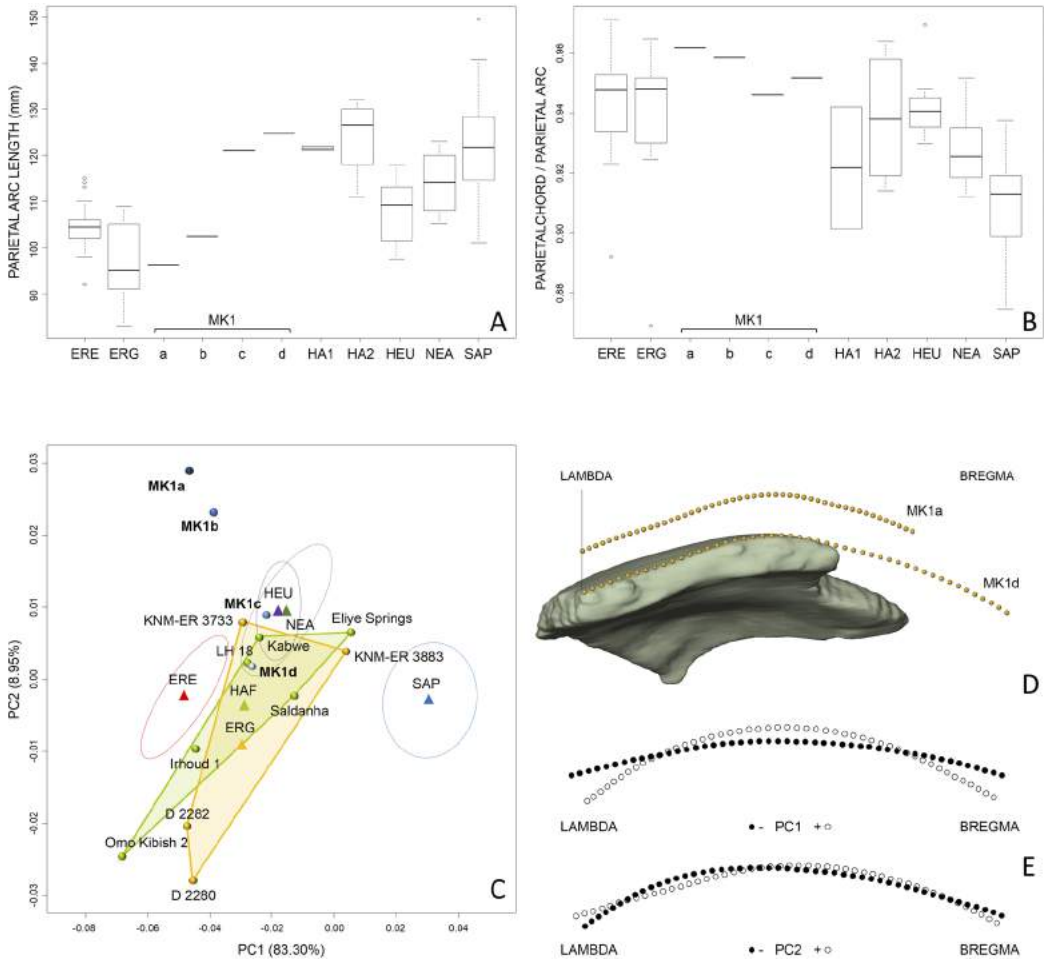

Fig. 6 - (A) Parietal arc length and (B) parietal curvature index in the OTUs reported in the Appendix; four different estimations for MK1 are shown: MK1a, MK1b, MK1c and MK1d (see text for details). C) PCA analysis (PC1 vs PC2) of landmark data taken on the mid-sagittal profile according to the configuration of landmarks "a" and "d" showed on the digital model of MK1 (D). E) Shape variations of the biparietal profile (from* lambda *to* bregma*) at the extremes of PC1 and PC2. The colour version of this figure is available at the JASs website.

two estimates corresponds more closely to the real morphology of the (complete) parietal from Gombore II, in agreement also with the result obtained exploring size and shape of the biparietal arc by traditional morphometrics. At the same time, the configurations MK1a and MK1b fall outside the more relevant fields of variability.

Frontal: inferior temporal line (shape analysis)

On the frontal (MK2), the inferior temporal line is preserved from the fronto-temporomalar (or *fmt*; i.e. the most external point of the zygomaticofrontal suture), but it does not reach *stephanion* (or *st*; i.e. the point where the inferior temporal line crosses the coronal suture).

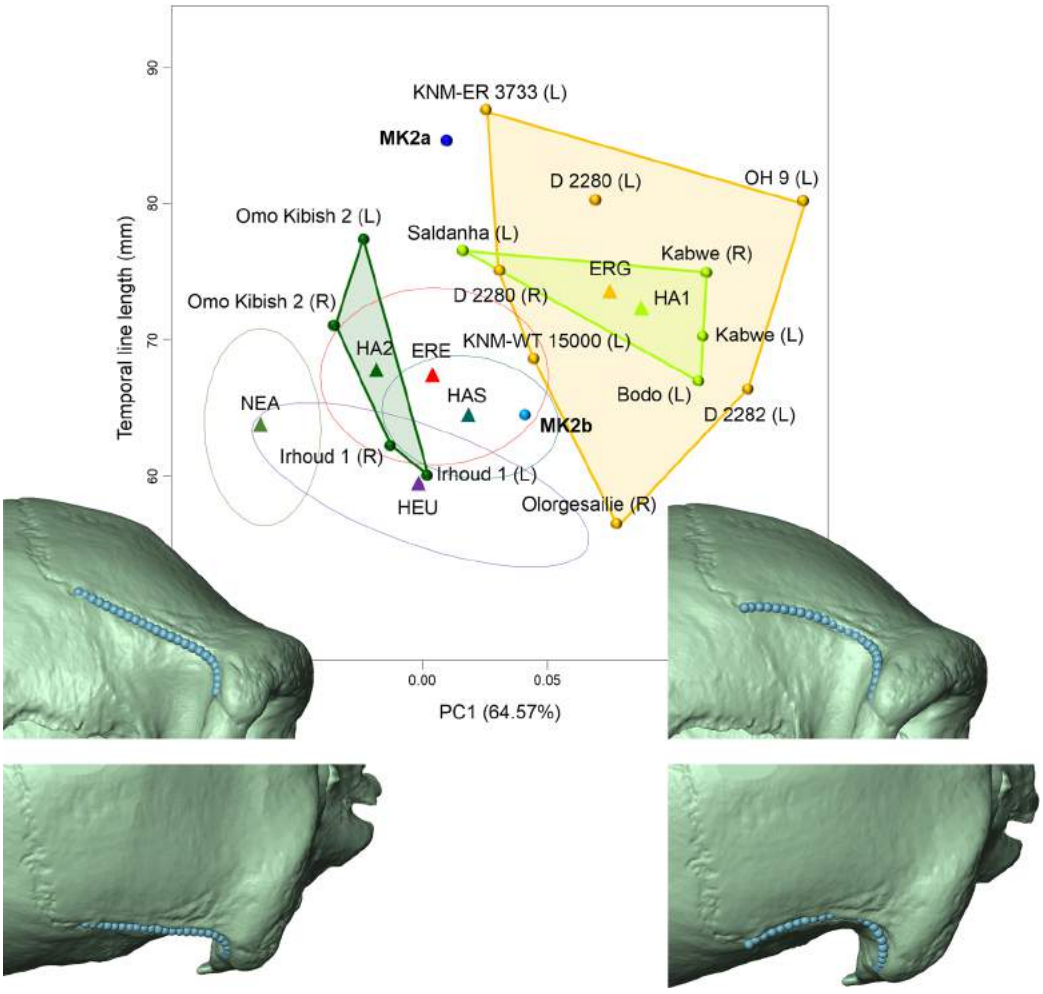

Fig. 7 - Bivariate plot comparing the variation in shape of the temporal line across the frontal bone (only PC1) and its total length in fossil human samples (OTUs and specimens as in Appendix); the estimated extended profiles of MK2 (see text for details) are respectively referred to as MK2a and MK2b. Consistent shape changes are showed on Kabwe 1 at the extreme poles of the PC1 extension. Legend as in the Appendix; L = left side; R = right side. The colour version of this figure is available at the JASs website.

The contour of the inferior temporal line was analysed using a set of 25 3D evenly-spaced landmarks (Fig. 7), estimating the *stephanion* in MK2 with a procedure similar to that used for the parietal arc. When possible, both right and left inferior temporal lines of the various specimens were sampled, mirroring the latter sub-sample before performing the analysis. Then, the Procrustes registration (function "procSym" of Morpho "R" package; Schlager, 2014) was performed. In MK2 the position of the *st* and the missing trait of the inferior temporal line were estimated two times (MK2a and MK2b), according to the mean length of two different species respectively: *Homo ergaster* and *Homo heidelbergensis*. In addition to MK2a and MK2b, the comparative

sample consists of 54 fossil specimens belonging to *Homo ergaster*, *Homo erectus*, *Homo heidelbergensis* (including the OTUs HA1 and HA2) and *Homo neanderthalensis* (see Appendix). Lengths of the inferior temporal line were measured through the function "bezierArcLength" of the bezier "R" package (Olsen, 2014).

In the PCA of the Procrustes coordinates, the first principal component explains 64.57% of the total variance; it has been plotted against the length of the inferior temporal lines (see Fig. 7). *Homo ergaster* is characterized in mean by a long temporal line despite the lower cranial size of this OTU with respect to the others (Holloway *et al.,* 2004); MK2a falls at the extreme of the variability of this species (ERG), whereas MK2b is close to that of HA1 (early African *Homo heidelbergensis*). It has to be underlined that, although the length of MK2a and MK2b configurations were respectively estimated on the ERG and HA1 median length, the missing landmarks were obtained independently from these length simulations.

Looking at the PC1 values only, MK2a falls near the centroid of *Homo erectus*, while MK2b is internal to the variability of both HA1 and ERG. This means that, as shown by the warpings of the line consistent to shape changes in the frontal region of a reference specimen (Fig. 7), either MK2a or MK2b exhibit moderate postorbital constriction.

Discussion and conclusions

An increasing body of data suggests that bipedal hominids engaged in the first out-of-Africa diffusion were not derived, encephalised and technologically advanced humans, but definitively more archaic creatures, with a brain just above 500 ml and a morphology close to that of the so-called "early *Homo*" (e.g., Rightmire *et al.*, 2006; Antón, 2012). The same corpus of data suggests that their dispersal started well before the appearance of the Acheulean, thus earlier than 1.6 Ma (see references in Manzi, 2012). Now we understand that – driven by ecological, rather than by behavioural or "cultural" motives – these earliest representatives of the genus *Homo* had the tendency to diffuse and adapt to variable non-tropical environments and that these dispersals were followed by geographical isolation. Under this approach, *Homo erectus* should be viewed as a species of the Far East, distributed in the island of Java and in Northern China, whereas its African counterparts may be regarded as a distinct species (*contra* Asfaw *et al.*, 2002), referred to as *Homo ergaster*, recognisable in the fossil record until about 1,0 Ma on the basis of specimens such as Daka, Buia and Olorgesailie (e.g., Manzi *et al.*, 2003; Manzi, 2004). At the same time, these crania of the late Early Pleistocene are distinct from those of the Middle Pleistocene that may be referred to *Homo heidelbergensis*, either in Africa (specimens like Bodo and Kabwe 1) in Europe (including the sample from Atapuerca SH, Petralona or Ceprano) or in mainland Asia (Narmada, Dali, Jinniushan).

These observations suggest a taxonomic and phylogenetic discontinuity that ranges across the Matuyama/Brunhes reversal of 780 ka, in possible relationship with the more general phenomenon known as the "Mid-Pleistocene revolution" (Maslin & Ridgwell, 2005) that, in turn, corresponds to the beginning of environmental changes related to the long and dramatic climatic breakdown of MIS 18-16. The phenetic distance between humans of the Early and the Middle Pleistocene in sub-Saharan Africa signals a crucial passage in the evolution of the genus *Homo* and probably represents a distinction at the species level. Although the period bracketed between approximately 900 and 600 ka is very poor of fossil evidence, it seems therefore that something crucial happened at that time, generating a new and more encephalised kind of humanity that spread quite rapidly in Africa and Eurasia. When viewed as a geographically widespread single taxon from which both Neanderthals and modern humans originated (e.g., Rightmire, 1998, 2008; Mounier *et al.*, 2009, 2011; Stringer, 2012), these humans of the Middle Pleistocene should be referred to as *Homo heidelbergensis* (Schoetensack, 1908), despite the scientific community still miss to find

an agreement on this point (e.g., Arsuaga *et al.*, 2014, 2015; Balter, 2014).

Nevertheless, at present, the chronology, topology and phylogenetic dynamics related to the rather synchronous appearance of Middle Pleistocene humans that we may refer to *Homo heidelbergensis* are still unclear. As a matter of fact, we do not know when and from where the humans that were ancestral to both the Neanderthals in Europe and *Homo sapiens* in Africa originated (Rightmire, 1998, 2008). A possible answer about the time of emergence of this last common ancestor comes from the complete mtDNA extracted from the phalanx of the Denisova cave in the Altai mountains, dated to 48-30 ka, which demonstrates the existence of humans that were different from both *Homo neanderthalensis* and *Homo sapiens*, but shared with them a common ancestor between 1.3 Ma and 779 ka (Krause *et al.*, 2010; Meyer *et al.,* 2012, 2014). As a working hypothesis, this suggests that the Denisova phalanx may represent a still unknown hominin that originated, together with the ancestor/s of Neanderthals and modern humans, before the beginning of the Middle Pleistocene and thus, interestingly, just before the appearance of *Homo heidelbergensis* in the fossil record. This scenario is integrated by inferences obtained when Neanderthals and modern humans are compared genetically. Their coalescence around 500 ka (Green *et al.*, 2008; Endicott *et al.*, 2010) is consistent with a more ancient common ancestor, as well as with the subsequent morphological divergence occurring between the European and African lineages during the Middle Pleistocene (as a number of studies demonstrated after Santa Luca, 1978).

Indeed, looking at the hypodigm of *Homo heidelbergensis* as a whole, it is clear that a considerable amount of variability characterises this species (Mounier *et al.*, 2009, 2011), since populations of Africa, Asia and Europe respectively bore peculiar regional features, promoting distinctions at the sub-specific level (as suggested by Manzi, 2012). Moreover, there is considerable phenotypic variation even within the same macro-region, at least across time. The variability of the European fossil record of the Middle Pleistocene, in particular, has been greatly expanded by the revised chronology of the calvarium from Ceprano in Italy (Muttoni *et al.*, 2009; Manzi *et al.*, 2010; Nomade *et al.*, 2011), a specimen that could document «the occurrence of an ancestral stock of *Homo heidelbergensis/rhodesiensis*» (Bruner & Manzi, 2007, p. 365), since it represents a mosaic morphological bridge between *Homo erectus* sensu lato, on one hand, and *Homo heidelbergensis*, on the other (Manzi *et al.*, 2001; Mounier *et al.*, 2011). Thus, despite its relatively recent age, the Italian specimen may represent the morphology of the yet undiscovered ancestral stock of *Homo heidelbergensis*, preserved in an isolated area of Southern Europe, while in other areas of the continent there the combination of derived features that characterise the so-called "Neanderthal lineage" was already appearing (e.g., Hublin, 2009; Manzi *et al.*, 2011; Arsuaga *et al.*, 2014).

Nevertheless, the best candidate for this crucial phylogenetic position should be more ancient than Ceprano and should not be in Europe. In this perspective, the fragmentary cranial remains from Gombore II (Melka Kunture, Ethiopia), respectively referred here to as MK1 (an incomplete left parietal) and MK2 (a right large frontal fragment), are in a privileged position in terms of both chronology (about 850 ka) and topology (sub-Saharan Eastern Africa). Our analysis supports the hypothesis that these distinct portions, probably belonging to the same heavy cranium (Fig. 8), demonstrate a morphology that is sufficiently distinct from *Homo ergaster*, despite the overlap of some features, and close to early representatives of African *Homo heidelbergensis*, particularly Kabwe 1 (or Broken Hill 1).

In support to this conclusion, we may underline the following points emerging from our present study:

1) both the parietal MK1 and the frontal MK2 should be referred to the genus *Homo* and, when combined, represent a single cranium (MK cranium) that exhibits an "archaic" morphology according to various features, including the degree and shape of the

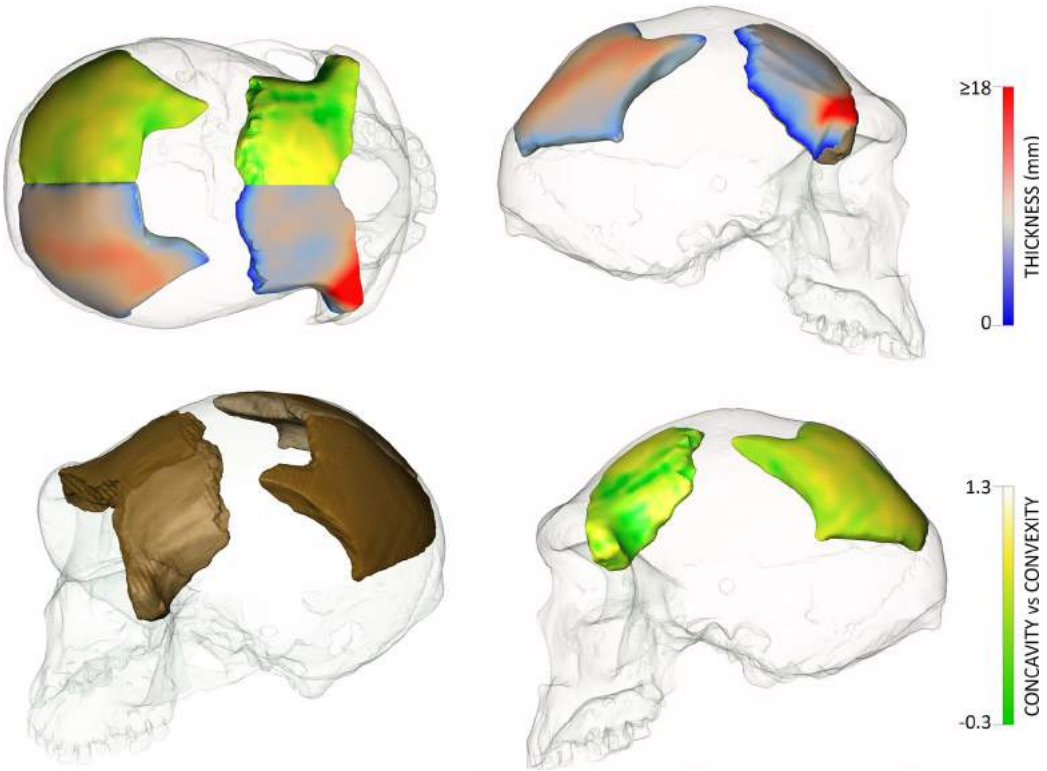

Fig. 8 - Virtual reconstruction of the MK cranium from Gombore II (MK1 + MK2), using a scaled version (0.96) of Kabwe 1. MK1 (left parietal) and MK2 (right frontal) are doubled by mirroring; colours representing the variation in thickness as well as the degree of curvature are reported (scales on the right); a more pictorial oblique view is also shown (bottom-left). The colour version of this figure is available at the JASs website.

curvature along both sagittal and transversal profiles, the absence of the parietal foramen, the development of the obelic branch of the middle meningeal vessels, the temporal lines that along the parietal run medially to the parietal eminence, the marked temporal lines on the frontal bone and the occurrence of a heavy frontal torus;

2) peculiar features of the MK cranium are both the remarkable thickness of the cranial bones – which is unusual among African specimens either of *Homo ergaster* or *Homo heidelbergensis*, whereas it is in common with Ceprano – and the strong divergence of the temporal lines behind the postorbital constriction;
3) it is rather obvious (but not without importance) that the MK cranium shows the greatest affinities with African demes (of both *Homo ergaster* and *Homo heidelbergensis*), while there are more clear distances with the Neanderthals and their European ancestors (HEU) as well as with *Homo sapiens* and, in part, with *Homo erectus;*
4) the parietal MK1 exhibits curvature and shape of the midsagittal profile that approximates *Homo ergaster* variability only when its arc length is elongated to values that are external to the same variability, whereas (given our estimation of the position of the *bregma*) it is closer to the field of variation of African *Homo*

heidelbergensis for absolute dimensions, degree of the curvature and shape;
5) MK1 has a strong and extended flattening of the obelic region on the external surface, very similar to that observed in Kabwe 1, and shows a marked depression of the endocast more laterally and anteriorly, where the thickness of the bone is higher than in other parts of the same parietal;
6) the consequently flattened parietal lobe of the endocast, combined with the dominance of the more posterior branches of the middle meningeal network, is a further feature that is shared among archaic varieties of the genus *Homo* in general (Bruner *et al.,* 2015);
7) in the frontal MK2, the shape of the inferior temporal line corresponds to the field of variability that is shared by *Homo ergaster* and early African *Homo heidelbergensis* (HA1);
8) MK2 does not show an extended lateral wing of the frontal torus, nor a strong postorbital constriction.

Given the affinities with African representatives of early *Homo heidelbergensis* (HA1) and particularly, as emerged from our results, with Kabwe 1, the MK cranial fragments were digitally placed on this specimen (see Fig. 8), in order to have an idea of their anatomical placement and emphasize the observed patterns of curvature and thickness. The alignment was performed using a landmark-based approach after scaling the landmark sets and the digital model belonging to Kabwe, using the parietal arc as scale factor (0.96). Following the same procedure, a restored virtual endocast of Kabwe was the guideline to estimate a probable cranial capacity of the MK cranium, which resulted to be around 1.080 cm^3.

In sum, we underline that the morphology of the MK specimens fills the phenetic gap observed between *Homo ergaster* and *Homo heidelbergensis*. In view of the chronology of the human cranial bones from Gombore II, this conclusion appears of extreme interest, suggesting that such a partial cranium represents at present the best, if not the unique candidate for the ancestral occurrence of *Homo heidelbergensis* around 800 ka, as well as an evidence that this species probably originated in Africa before its dispersal in Eurasia.

Acknowledgements

Our gratitude goes to the Direction and Curators of the National Museum of Ethiopia in Addis Ababa for the permission to study the human fossil specimens labelled MK73 / GOM II – 6769 and MK76 / GOM II – 576 (respectively MK1 and MK2) and for their guidance and support in the laboratory. We are also grateful to the Authorities of the Oromia Region of Ethiopia as well as to the Ethiopian Archaeological Service. We acknowledge and thank several people for providing access to comparative material and/or for useful discussions; particularly Markus Bastir, Carmine Collina, Alfredo Coppa and the Eritrean-Italian Danakil Expedition (Anthropo-Archaeological and Geo-Paleontological Mission), Rosalia Gallotti, David Lordkipanidze, the NESPOS Society, Tom Plummer, Ian Tattersall, as well as the Editor of the JASs and the Guest-editors of this Proceeding Paper section. This research was partially supported by Sapienza University of Rome, particularly with the Award C26H13A45J credited in 2013 to the project "Human evolution and environment" led by one of us (GM).

References

Abbate E., Albianelli A., Azzaroli A., Benvenuti M., Tesfamariam B., Bruni P., Cipriani N., Clarke R.J., Ficcarelli G. & Macchiarelli R. 1998. A one-million-year-old *Homo* cranium from the Danakil (Afar) Depression of Eritrea. *Nature,* 393: 458-460.

Antón S.C. 2012. Early *Homo*: Who, When, and Where. *Curr. Anthropol.*, 53: S278-S298.

Arbour J.H. & Brown C.M. 2014. Incomplete specimens in geometric morphometric analyses. *Methods Ecol. Evol.*, 5: 16-26.

Arsuaga J.L., Martínez I., Arnold L.J., Aranburu A., Gracia-Téllez A., Sharp W.D., Quam R.M.,

Falguères C., Pantoja-Pérez A., Bischoff J., Poza-Rey E., Parés J.M., Carretero J.M., Demuro M., Lorenzo C., Sala N., Martinón-Torres M., García N., Alcázar de Velasco A., Cuenca-Bescós G., Gómez-Olivencia A., Moreno D., Pablos A., Shen C.C., Rodríguez L., Ortega A.I., García R., Bonmatí A., Bermúdez de Castro J.M. & Carbonell E. 2014. Neandertal roots: Cranial and chronological evidence from Sima de los Huesos. *Science*, 344: 1358-1363.

Arsuaga J.L., Carretero J.-M., Lorenzo C., Gómez-Olivenci, A., Pablos A., Rodríguez L., García-González R., Bonmatí A., Quam R.M., Pantoja-Pérez A., Martínez I., Aranburu A., Gracia-Téllez A., Poza-Rey E., Sala N., García N., Alcázar de Velasco A., Cuenca-Bescós G., Bermúdez de Castro J.M. & Carbonell E. 2015. Postcranial morphology of the middle Pleistocene humans from Sima de los Huesos, Spain. *Proc. Natl. Acad. Sci. USA,* 112: 11524-11529.

Ascenzi A., Mallegni F., Manzi G., Segre A.G. & Naldini E.S. 2000. A re-appraisal of Ceprano calvaria affinities with *Homo erectus*, after the new reconstruction. *J. Hum. Evol.,* 39: 443-450.

Asfaw B., Gilbert W.H., Beyene Y., Hart W.K., Renne P.R., WoldeGabriel G., Vrba E.S. & White T.D. 2002. Remains of *Homo erectus* from Bouri Middle Awash Ethiopia. *Nature,* 416: 317-320.

Asfaw B., Gilbert W.H. & Richards G.D. 2008. *Homo erectus* Cranial Anatomy. In W.H. Gilbert & B. Asfaw (eds): Homo erectus: *Pleistocene Evidence from the Middle Awash, Ethiopia,* pp. 365-328. University of California Press, Los Angeles & London.

Balter M. 2014. RIP for a key *Homo* species? *Science,* 345: 129-129.

Bermudez de Castro J.M., Arsuaga J.L., Carbonell E., Rosas A., Martìnez I. & Mosquera M. 1997. A hominid from the Lower Pleistocene of Atapuerca Spain: possible ancestor to Neandertals and modern humans. *Science,* 276: 1392-1395.

Bonnefille R. 1972. *Association polliniques actuelles et quaternaires en Ethiopie (vallées de l'Awash et de l'Omo).* PhD thesis, University of Paris VI, Paris.

Bruner E., Grimaud-Hervé D., Wu X., de la Cuétara J.M. & Holloway R. 2015. A paleoneurological survey of Homo erectus endocranial metrics. *Quat. Int.,* 368: 80-87.

Bruner E. & Manzi G. 2007. Landmark-based shape analysis of the archaic *Homo* calvarium from Ceprano (Italy). *Am. J. Phys. Anthropol.,* 132: 355-366.

Chavaillon J. 1979. Un site acheuléen près du lac Langano, (Ethiopie). *Abbay*, 10: 57–74.

Chavaillon J. & Berthelet A. 2004. The archaeological sites of Melka Kunture. In M. Piperno & J. Chavaillon (eds): *Studies on the Early Paleolithic site of Melka Kunture, Ethiopia*, pp. 25-80. Istituto Italiano di Preistoria e Protostoria, Florence.

Chavaillon J., Brahimi C. & Coppens Y. 1974, Première découverte d'Hominidé dans l'un des sites acheuléens de Melka-Kunturé (Ethiopie). *C.R. Acad. Sci. Paris,* 278: 3299-3302.

Chavaillon J. & Coppens Y. 1975. Découverte d'Hominidé dans un site acheuléen de Melka-Kunturé. *Bull. Mém. Soc. Anthropol. Paris,* 2: 125–128

Chavaillon J. & Coppens Y. 1986. Nouvelle découverte d'*Homo erectus* à Melka-Kunturé. *C.R. Acad. Sci. Paris,* 303: 99-104.

Coppens Y. 2004. The hominids of Melka Kunture. Some general reflections. In M. Piperno & J. Chavaillon (eds): *Studies on the Early Paleolithic site of Melka Kunture, Ethiopia*, pp. 685-686. Istituto Italiano di Preistoria e Protostoria, Florence.

Cunningham D.J. 1908. The Evolution of the Eyebrow Region of the Forehead, with Special Reference to the Excessive Supraorbital Development in the Neanderthal Race. *Trans. R. Soc. Edinb.,* 46: 283-310.

Di Vincenzo F., Rodriguez L., Carretero J.M., Collina C., Geraads D., Piperno M. & Manzi G. 2015. The massive fossil humerus from the Oldowan horizon of Gombore I, Melka Kunture (Ethiopia, >1.39 Ma). *Quat. Sci. Rev.,* 122: 207-221.

Endicott P., Ho S.Y.W. & Stringer C. 2010. Using genetic evidence to evaluate four palaeoanthropological hypotheses for the timing

of Neanderthal and modern human origins. *J. Hum. Evol.,* 59: 87-95.

Gallotti R., Collina C., Raynal J.-P., Kieffer G., Geraads D. & Piperno M. 2010. The early Middle Pleistocene site of Gombore II (Melka Kunture, Upper Awash, Ethiopia) and the issue of Acheulean bifacial shaping strategies. *Afr. Archaeol. Rev.,* 27: 291-322.

Geraads D. 1979. La faune des gisements de Melka-Kunturé: artiodactyles, primates. *Abbay*, 10: 21-50.

Geraads D. 1985. La faune des gisements de Melka-Kunturé (Ethiopie). In M. Beden, A. K. Behrensmeyer, N. T. Boaz, R. Bonnefille, C. K. Brain, B. Cooke, Y. Coppens, R. Dechamps,V. Eisenmann, A. Gentry, D. Geraads, R. Gèze, C. Guérin, J. Harris, J-C. Koeniguer, R. Letouzey, G.Petter, A. Vincens & E. Vrba (eds): *L'environnement des Hominidés au Plio-Pleistocène,* pp.165-174. Masson, Paris.

Green R.E., Malaspinas A.-S., Krause J., Briggs A.W., Johnson P.L.F., Uhler C., Meyer M., Good J.M., Maricic T., Stenzel U., Prüfer K., Siebauer M., Burbano H.A., Ronan M., Rothberg J.M., Egholm M., Rudan P., Brajković D., Kućan Z., Gusić I., Wikström M., Laakkonen L., Kelso J., Slatkin M. & Pääbo S. 2008. A complete Neandertal mitochondrial genome sequence determined by high-throughput sequencing. *Cell*, 134: 416-426.

Haile-Selassie Y., Asfaw B. & White T.D. 2004. Hominid cranial remains from upper Pleistocene deposits at Aduma, Middle Awash, Ethiopia. *Am. J. Phys. Anthropol.*, 123: 1-10.

Holloway R.L., Broadfield D.C. & Yuan M.S.T. 2004. *The Human Fossil Record: Brain Endocasts the Paleoneurological Evidence*. Wiley-Liss, New York.

Hublin J.-J. 2009. The origin of Neandertals. *Proc. Natl. Acad. Sci. USA,* 106: 16022–16027.

Kaifu Y., Aziz F., Indriati E., Jacob T., Kurniawan I. & Baba H. 2008. Cranial morphology of Javanese *Homo erectus*: new evidence for continuous evolution, specialization, and terminal extinction. *J. Hum. Evol.*, 55: 551-580.

Krause J., Fu Q., Good J.M., Viola B., Shunkov M.V., Derevianko A.P. & Pääbo S. 2010. The complete mitochondrial DNA genome of an unknown hominin from southern Siberia. *Nature,* 464: 894-897.

Lordkipanidze D., Vekua A., Ferring R., Rightmire G.P., Zollikofer C.P., Ponce de León M.S., Agusti J., Kiladze G., Mouskhelishvili A., Nioradze M. & Tappen M. 2006. A fourth hominin skull from Dmanisi, Georgia. *Anat. Rec. A*, 288: 1146-1157.

Macchiarelli R., Bondioli L., Chech M., Coppa A., Fiore I., Russom R., Vecchi F., Libsekal Y. & Rook L. 2004. The late Early Pleistocene human remains from Buia, Danakil depression, Eritrea. *Rivista Italiana di Paleontologia e Stratigrafia,* 110: 133-144.

Manzi G. 2004. Human evolution at the Matuyama/Brunhes boundary. *Evol. Anthropol.*, 13: 11-24.

Manzi G. 2012. On the trail of the genus *Homo* between archaic and derived morphologies. *J. Anthropol. Sci.,* 90: 1-18.

Manzi G., Bruner E. & Passarello P. 2003. The one-million-year-old *Homo* cranium from Bouri (Ethiopia): a reconsideration of its *H. erectus* affinities. *J. Hum. Evol.*, 44: 731-736.

Manzi G., Magri D., Milli S., Palombo M.R., Margari V., Celiberti V., Barbieri M., Barbieri M., Melis R.T., Rubini M., Ruffo M., Saracino B., Tzedakis P.C., Zarattini A. & Biddittu I. 2010. The new chronology of the Ceprano calvarium (Italy). *J. Hum. Evol.,* 59: 580-585.

Manzi G., Magri D. & Palombo M.R. 2011. Early-Middle Pleistocene environmental changes and human evolution in the Italian peninsula. *Quat. Sci. Rev*. 30: 1420-1438.

Manzi G., Mallegni F. & Ascenzi A. 2001. A cranium for the earliest Europeans: phylogenetic position of the hominid from Ceprano, Italy. *Proc. Natl. Acad. Sci. USA,* 98: 10011-10016.

Maslin M.A. & Ridgwell A.J. 2005. Mid-Pleistocene revolution and the 'eccentricity myth'. In M.J. Head & P.L. Gibbard (eds): *Early Middle Pleistocene Transition: The Land-Ocean Evidence*, pp. 19-34. Geological Society, Special Publications Vol. 247, London.

Meindl R.S. & Lovejoy C.O. 1985. Ectocranial suture closure: A revised method for the

determination of skeletal age at death based on the lateral-anterior sutures. *Am. J. Phys. Anthropol.,* 68: 57-66.

Meyer M., Kircher M., Gansauge M.-T., Li H., Racimo F., Mallick S., Schraiber J.G., Jay F., Prüfer K., de Filippo C., Sudmant P.H., Alkan C., Fu Q., Do R., Rohland N., Arti Tandon Siebauer M., Green R.E., Bryc K., Briggs A.W., Stenzel U., Dabney J., Shendure J., Kitzman J., Hammer M.F., Shunkov M.V., Derevianko A.P., Patterson N., Andrés A.M., Eichler E.E., Slatkin M., Reich D., Kelso J. & Pääbo S. 2012. A high-coverage genome sequence from an archaic Denisovan individual. *Science*, 338: 222-226.

Meyer M., Fu Q., Aximu-Petri A., Glocke I., Nickel B., Arsuaga J.-L., Martinez I., Gracia A., Bermudez de Castro J.M., Carbonell E. & Pääbo S. 2014. A mitochondrial genome sequence of a hominin from Sima de los Huesos. *Nature*, 505: 403-406.

Morgan L.E., Renne P.R., Kieffer G., Piperno M., Gallotti R. & Raynal J.-P. 2012. A chronological framework for a long and persistent archaeological record: Melka Kunture, Ethiopia. *J. Hum. Evol.*, 62: 104-115.

Mounier A., Marchal F. & Condemi S. 2009. Is *Homo heidelbergensis* a distinct species? New insight on the Mauer mandible. *J. Hum. Evol.,* 56: 219-246.

Mounier A., Condemi S. & Manzi G. 2011. The stem species of our species: a place for the archaic human cranium from Ceprano Italy. *PloS One,* 6: e18821.

Muttoni G., Scardia G., Kent D.V., Swisher C.C. & Manzi G. 2009. Pleistocene magnetochronology of early hominin sites at Ceprano and Fontana Ranuccio, Italy. *Earth Planet Sci. Lett.*, 286: 255-268.

Nomade S., Muttoni G., Guillou H., Robin E. & Scardia G., 2011. First ^{40}Ar/^{39}Ar age of the Ceprano man (central Italy). *Quartern. Geochronol.*, 6: 453-457.

Oakley K.P., Campbell B.G. & Molleson T.I. (eds). 1977. *Catalogue of Fossil Hominids. Part I: Africa (2nd Edition)*. Trustees of the British Museum (Natural History), London.

Olsen A. 2014. Bezier: Bezier Curve and Spline Toolkit. *R Package Version 1.1*.

Potts R., Behrensmeyer A.K., Deino A., Ditchfield P. & Clark J. 2004. Small Mid-Pleistocene Hominin Associated with East African Acheulean Technology. *Science,* 305: 75-78.

Profico A. & Veneziano A. 2015. Arothron: R Functions for Geometric Morphometrics Analyses. R package version 314 1.0 http://github.com/Arothron/Arothron, doi:10.5281/*zenodo*.28194.

Raynal J.-P., Kieffer G. & Bardin G. 2004. Garba IV and the Melka Kunture Formation. A preliminary lithostratigraphic approach. In M. Piperno & J. Chavaillon (eds): *Studies on the Early Paleolithic site of Melka Kunture, Ethiopia*, pp. 137-166. Istituto Italiano di Preistoria e Protostoria, Florence.

Rightmire G.P. 1998. Human evolution in the Middle Pleistocene: The role of *Homo heidelbergensis*. *Evol. Anthropol.,* 6: 218-227.

Rightmire G.P. 2008. *Homo* in the Middle Pleistocene: hypodigms, variation, and species recognition. *Evol. Anthropol.*, 17: 8-21.

Rightmire G.P. 2009. Middle and later Pleistocene hominins in Africa and Southwest Asia. *Proc. Natl. Acad. Sci. USA,* 106: 16046-16050.

Rightmire G.P. 2013. *Homo erectus* and Middle Pleistocene hominins: brain size, skull form, and species recognition. *J. Hum. Evol.*, 65: 223-252.

Rightmire G.P., Lordkipanidze D. & Vekua A. 2006. Anatomical descriptions, comparative studies and evolutionary significance of the hominin skulls from Dmanisi, Republic of Georgia. *J. Hum. Evol.,* 50: 115-141.

Saban R. 1995. Image of the human fossil brain: endocranial casts and meningeal vessels in young and adult subjects In J.-P. Changeux & J. Chavaillon (eds): *Origins of the human brain*, pp. 11-41. Oxford University Press, Oxford.

Santa Luca A.P. 1978. A re-examination of presumed Neandertal-like fossils. *J. Hum. Evol.,* 7: 619-636.

Santa Luca A.P. 1980. *The Ngandong fossil hominids: a comparative study of a far eastern* Homo erectus *group*. Yale University Press, New Haven.

Schlager S. 2014. Morpho: Calculations and visualisations related to Geometric Morphometrics. *R Package Version 2.2.*

Schwartz J.H. & Tattersall I. 2005. *The human fossil record, craniodental morphology of genus* Homo *(Africa and Asia)*. John Wiley & Sons, New York.

Shoetensack O. 1908. *Der Unterkiefer des* Homo heidelbergensis*, aus den Sanden von Mauer bei Heidelberg*. Wilhelm Englemann, Leipzig.

Stringer C. 2012. The status of *Homo heidelbergensis* (Schoetensack 1908). *Evol. Anthropol.,* 21: 101-107.

Tamrat E., Thouveny N., Taieb M. & Brugal J.P. 2014. Magnetostratigraphic study of the Melka Kunture archaeological site (Ethiopia) and its chronological implications. *Quat. Int*. 343: 5-16.

White M.J. 1998. Twisted ovate bifaces in the British Lower Palaeolithic: Some observations and implications. In N. Ashton, F. Healy & P. Pettitt (eds): *Stone age archaeology: Essays in honor of John Wymer*, pp. 98–104. Lithic Studies Society Occasional Paper, 6, London.

Appendix - Specimens sampled and sources of metric data.

SPECIMEN	SPECIES	OTU	PARIETAL			FRONTAL (INF. TEMPORAL LINE)
			ARC	CHORD	GMM	GMM
Melka Kunture 1		MK1a	*	*	-	-
		MK1b	*	*	-	-
		MK1c	*	*	-	-
		MK1d	*	*	-	-
Melka Kunture 2		MK2a	-	-	-	R
		MK2b	-	-	-	R
Bukuran	*Homo erectus*	ERE	a	a	-	-
Ngandong 1	*Homo erectus*	ERE	b	b	-	-
Ngandong 10	*Homo erectus*	ERE	b	b	-	-
Ngandong 11	*Homo erectus*	ERE	b	b	-	-
Ngandong 12	*Homo erectus*	ERE	b	b	**	R/L
Ngandong 3	*Homo erectus*	ERE	b	b	-	-
Ngandong 5	*Homo erectus*	ERE	b	b	-	-
Ngandong 6	*Homo erectus*	ERE	b	b	-	-
Ngandong 7	*Homo erectus*	ERE	b	b	**	R
Ngandong 9	*Homo erectus*	ERE	b	b	-	-
Sambungmacan 1	*Homo erectus*	ERE	a	a	-	-
Sambungmacan 3	*Homo erectus*	ERE	a	a	**	R/L
Sambungmacan 4	*Homo erectus*	ERE	a	a	-	-
Sangiran 10	*Homo erectus*	ERE	a	a	-	-
Sangiran 12	*Homo erectus*	ERE	a	a	-	-
Sangiran 17	*Homo erectus*	ERE	b	b	-	-
Sangiran 2	*Homo erectus*	ERE	c	c	**	L
Sangiran 38	*Homo erectus*	ERE	a	a	-	-
Sangiran IX (Tjg-1993.05)	*Homo erectus*	ERE	f	-	-	-
Zhoukoudian II	*Homo erectus*	ERE	-	-	**	-
Zhoukoudian III	*Homo erectus*	ERE	-	-	**	R/L
Zhoukoudian X	*Homo erectus*	ERE	c	c	**	-

Appendix (continued).

SPECIMEN	SPECIES	OTU	PARIETAL			FRONTAL (INF. TEMPORAL LINE)
			ARC	CHORD	GMM	GMM
Zhoukoudian XI	*Homo erectus*	ERE	c	c	**	R/L
Zhoukoudian XII	*Homo erectus*	ERE	c	c	**	-
Buia (UA 31)	*Homo ergaster*	ERG	*	*	-	-
D2280	*Homo ergaster*	ERG	d	d	**	R/L
D2282	*Homo ergaster*	ERG	d	d	**	L
D2700	*Homo ergaster*	ERG	d	d	-	-
D3444	*Homo ergaster*	ERG	e	e	-	-
Daka (BOU-VP-2/66)	*Homo ergaster*	ERG	i	i	-	-
KNM-ER 42700	*Homo ergaster*	ERG	f	-	-	-
KNM-ER-3733	*Homo ergaster*	ERG	c	c	**	L
KNM-ER-3883	*Homo ergaster*	ERG	c	c	**	-
KNM-WT 15000	*Homo ergaster*	ERG	d	d	-	L
OH9	*Homo ergaster*	ERG	-	-	-	L
Olorgesailie	*Homo ergaster*	ERG	-	-	-	R
Kabwe 1	*Homo heidelbergensis*	HA1	b	b	**	R/L
Bodo	*Homo heidelbergensis*	HA1	-	-	-	L
Dali	*Homo heidelbergensis*	HAS	-	-	-	R/L
Zuttiyeh	*Homo heidelbergensis*	HAS	-	-	-	R/L
Saldanha	*Homo heidelbergensis*	HA1	g	g	**	L
Eliye Springs (KNM-ES 11693)	*Homo heidelbergensis*	HA2	h	h	**	-
Narmada	*Homo heidelbergensis*	HAS	-	-	-	R
Irhoud 1	*Homo heidelbergensis*	HA2	h	h	**	R/L
Ngaloba (LH 18)	*Homo heidelbergensis*	HA2	h	h	**	-
Omo Kibish 2	*Homo heidelbergensis*	HA2	g	g	**	R/L
Arago XXI/XLVII	*Homo heidelbergensis*	HEU	g	g	-	R/L
Ceprano	*Homo heidelbergensis*	HEU	*	*	-	L
Petralona	*Homo heidelbergensis*	HEU	g	g	**	R/L
Atapuerca Sima de los Huesos 4	*Homo heidelbergensis*	HEU	g	g	**	R/L

Appendix (continued).

SPECIMEN	SPECIES	OTU	PARIETAL			FRONTAL (INF. TEMPORAL LINE)
			ARC	CHORD	GMM	GMM
Atapuerca Sima de los Huesos 5	*Homo heidelbergensis*	HEU	g	g	**	-
Stenheim	*Homo heidelbergensis*	HEU	*	*	**	R
Swascombe	*Homo heidelbergensis*	HEU	*	*	**	-
Amud	*Homo neanderthalensis*	NEA	*	*	**	R/L
Gibraltar 1	*Homo neanderthalensis*	NEA	-	-	-	R
Guattari 1	*Homo neanderthalensis*	NEA	*	*	**	L
La Chapelle-aux-Saints	*Homo neanderthalensis*	NEA	b	b	**	R/L
La Ferrassie 1	*Homo neanderthalensis*	NEA	b	b	**	L
Neanderthal 1 (Feldhofer)	*Homo neanderthalensis*	NEA	-	-	-	L
La Quina 5	*Homo neanderthalensis*	NEA	b	b	-	R/L
Shanidar 1	*Homo neanderthalensis*	NEA	-	-	-	R
Saccopastore 1	*Homo neanderthalensis*	NEA	*	*	**	-
Spy1	*Homo neanderthalensis*	NEA	b	b	**	R
Spy2	*Homo neanderthalensis*	NEA	b	b	**	R/L
Tabun C1	*Homo neanderthalensis*	NEA	b	b	-	R/L
CSIC-OL 1068	*Homo sapiens*	SAP	*	*	**	-
CSIC-OL 794	*Homo sapiens*	SAP	*	*	**	-
CSIC-OL 866	*Homo sapiens*	SAP	*	*	**	-
CSIC-OL 886	*Homo sapiens*	SAP	*	*	**	-
CSIC-OL1112	*Homo sapiens*	SAP	*	*	**	-
CSIC-OL1187	*Homo sapiens*	SAP	*	*	**	-
CSIC-OL1192	*Homo sapiens*	SAP	*	*	**	-
CSIC-OL1193	*Homo sapiens*	SAP	*	*	**	-
CSIC-OL1197	*Homo sapiens*	SAP	*	*	**	-
CSIC-OL1199	*Homo sapiens*	SAP	*	*	**	-
CSIC-OL1282	*Homo sapiens*	SAP	*	*	**	-
CSIC-OL1428	*Homo sapiens*	SAP	*	*	**	-
VA-003-CR	*Homo sapiens*	SAP	*	*	**	-

Appendix (continued).

SPECIMEN	SPECIES	OTU	PARIETAL			FRONTAL (INF. TEMPORAL LINE)
			ARC	CHORD	GMM	GMM
VA-004-CR	*Homo sapiens*	SAP	*	*	**	-
VA-005-CR	*Homo sapiens*	SAP	*	*	**	-
VA-006-CR	*Homo sapiens*	SAP	*	*	**	-
VA-010-CR	*Homo sapiens*	SAP	*	*	**	-
VA-011-CR	*Homo sapiens*	SAP	*	*	**	-
VA-012-CR	*Homo sapiens*	SAP	*	*	**	-
VA-013-CR	*Homo sapiens*	SAP	*	*	**	-
VA-014-CR	*Homo sapiens*	SAP	*	*	**	-
VA-016-CR	*Homo sapiens*	SAP	*	*	**	-
VA-017-CR	*Homo sapiens*	SAP	*	*	**	-
VA-020-CR	*Homo sapiens*	SAP	*	*	**	-
VA-021-CR	*Homo sapiens*	SAP	*	*	**	-
VA-022-CR	*Homo sapiens*	SAP	*	*	**	-
VA-023-CR	*Homo sapiens*	SAP	*	*	**	-
VA-024-CR	*Homo sapiens*	SAP	*	*	**	-
VA-026-CR	*Homo sapiens*	SAP	*	*	**	-
VA-027-CR	*Homo sapiens*	SAP	*	*	**	-
VA-029-CR	*Homo sapiens*	SAP	*	*	**	-
VA-030-CR	*Homo sapiens*	SAP	*	*	**	-
VA-031-CR	*Homo sapiens*	SAP	*	*	**	-
VA-032-CR	*Homo sapiens*	SAP	*	*	**	-

* The parietal arc and chord values were acquired on original specimen, cast or 3D model, when not available in the literature: a: Kaifu *et al.*, 2008; b: Santa Luca, 1980; c: Ascenzi *et al.*, 2000; d: Rightmire *et al.*, 2006; e: Lordkipanidze *et al.*, 2006; f: Rightmire, 2013; g: Rightmire, 2008; h: Haile-Selassie *et al.,* 2004; i: Asfaw *et al.,* 2008.

** Specimen sampled for GMM analysis of the midsagittal curvature between *lambda* and *bregma*.
R/L Right and/or Left side of the specimen that was sampled for GMM analysis of the inferior temporal line along the frontal bone.